BEACH SAND-DERIVED MESOPOROUS SILICA BY HYDROTHERMAL PROCESS FOR HYDROCRACKING WASTE COCONUT OIL TO BIOFUEL

Siti Salamah[1], Farrah Fadhillah Hanum[1]*, Wega Trisunaryati[2], Indriana Kartini[2] and Suryo Purwono[3]

[1]Departement of Chemical Engineering, Faculty of Industrial Technology, Universitas Ahmad Dahlan, Yogyakarta, Indonesia
[2]Departement of Chemistry, Faculty of Mathematics and Natural Sciences, Universitas Gadjah Mada, Yogyakarta, Indonesia
[3]Departement of Chemical Engineering, Faculty of Engineering, Universitas Gadjah Mada, Yogyakarta, Indonesia

ARTICLE INFO	ABSTRACT
  	Hydrocracking, a key process for converting waste coconut oil into biofuel, requires efficient catalysts. This study investigates the synthesis of mesoporous silica catalysts using a hydrothermal process. Dodecyl amine, sourced from beach sand, serves as a template. The hydrothermal synthesis involved durations (12, 15, 18, 21, and 24 hours) and dodecyl amine concentrations (0.25 M, 0.5 M, 0.1 M), conducted at 40 °C for 30 minutes. The synthesized catalysts were then characterized for their surface area, pore volume, and diameter. Among the synthesized samples, those treated for 15 hours displayed optimal total acidity at 0.88 mmol/g. The catalysts synthesized with a dodecyl amine concentration of 0.025 M exhibited superior characteristics, including a specific surface area of 233 m²/g, a pore volume of 0.47 cc/g, and an average pore diameter of 2.10 nm. These findings underscore the efficacy of mesoporous silica catalysts in hydrocracking, particularly in converting large hydrocarbon molecules into smaller, more valuable biofuel molecules. Comparative analysis with similar research highlights the significance of these findings in the field of sustainable energy. The optimal catalyst conditions yielded a liquid fraction of over 70% for 0.25 M dodecyl amine. This efficiency in converting waste coconut oil into biofuel signifies the potential of mesoporous silica catalysts in advancing environmentally friendly energy sources. This research contributes to the growing knowledge of renewable energy, offering promising avenues for developing sustainable and eco-friendly energy solutions..

INTRODUCTION

Hydrocracking is a process that involves breaking down large hydrocarbon molecules into smaller ones by using hydrogen gas and a catalyst. Waste coconut oil contains large hydrocarbon molecules that cannot be used as biofuel. Hydrocracking breaks down these large molecules into smaller ones that can be biofueled [1]. The production of biofuel from leftover coconut oil has various advantages for the environment and the economy. Because biofuels are renewable and emit fewer emissions when burned, they have the environmental benefit of reducing greenhouse gas emissions and

dependency on fossil fuels [2]. From an economic standpoint, it can lower waste disposal costs and open new revenue sources for businesses producing waste coconut oil. Additionally, by varying fuel sources, it can improve energy security. These advantages coincide with the global movement toward environmentally friendly energy and waste disposal methods.

Optimizing the hydrocracking process necessitates the use of catalysts. Research indicates that catalysts for biofuel hydrocracking vary based on the feedstock type, with key characteristics like porosity, surface area, and crystal size significantly impacting their effectiveness [3,4]. Mesoporous silica, with its orderly, interconnected pore network ranging from 2 to 50 nanometers, is vital in hydrocracking [5]. Its structural properties, including a high surface area and controlled pore size distribution, make mesoporous silica an excellent support material for hydrocracking catalysts, enhancing reactant accessibility to the catalytic species [6–8].

Mesoporous materials are characterized by a large specific surface area and pore volume, often exhibiting a hexagonally mesostructured arrangement, making them useful as adsorbents and catalysts [9,10]. Silica, a key component in producing mesoporous materials, can be sourced synthetically or naturally [9,11]. An alternative source for silica is beach sand, a sustainable, abundant, and globally available resource ideal for synthesizing mesoporous silica catalysts. Among various mesoporous silica materials, SBA-15 stands out for its advantages in catalysis and as a catalyst support [8].

In this study, beach sand silica is utilized to enhance the economic value of this abundant resource. Beach sand is rich in silica

oxide (SiO_2), making it a suitable candidate for mesoporous material production. Mesoporous SiO_2 materials, as noted in previous research, have larger pore sizes compared to microporous materials, making them suitable for applications in catalysts and adsorbents [12]. The transition from microporous to mesoporous materials offers benefits like improved thermal stability, increased resistance to deactivation, enhanced acid activity, better ion exchange capabilities, and superior shape selectivity, all important for catalytic activity, particularly given the mass transfer limitations associated with small micropores [5].

The hydrothermal process is increasingly recognized as an effective method for synthesizing mesoporous silica [5,10,13]. This process, preferred over methods like sonochemistry for its simplicity and cost-effectiveness, allows for control over pore diameter by adjusting the hydrothermal treatment duration, influencing specific surface area, pore volume, and pore size distribution [10].

The synthesized mesoporous silica is prepared by employing dodecyl amine as a template. The resulting mesoporous silica is employed in hydrocracking used cooking oil, aiming to convert it into renewable fuels, thereby addressing the increasing quantity of used cooking oil. Using mesoporous silica catalysts in the hydrocracking of waste coconut oil to biofuel contributes to developing sustainable and environmentally friendly energy sources. Converting waste coconut oil into biofuel reduces dependence on non-renewable resources and helps mitigate greenhouse gas emissions. By varying the hydrothermal time and dodecyl amine concentration, this research aims to optimize the properties and performance of the synthesized mesoporous silica catalyst. The characterization

and evaluation of the catalyst will provide valuable insights into its potential application in the hydrocracking process of waste coconut oil to produce biofuel. Used cooking oil primarily consists of six compounds, among which petroselinic and palmitic acid are the major constituents. In the hydrocracking process, these compounds are converted into shorter hydrocarbon chains [14]. Hydrocracking of used cooking oil not only aids in utilizing food industry waste but also promotes environmental conservation [15].

Previous research has shown that the hydrotreatment of used coconut oil using a NiMo/NH_2-MS catalyst resulted in a liquid fraction yield of 77.9% [16]. Related studies include the synthesis and characterization of a Ni-NH2/mesoporous silica catalyst derived from Lapindo mud for hydrocracking waste cooking oil into biofuel [8,17,18]. The current study focuses on employing mesoporous silica for the hydrocracking of used cooking oil. The mesoporous silica used in this research is sourced from beach sand and synthesized hydrothermally at 100 °C, using dodecyl amine (DDA) as a template.

METHODS

1.Materials

Sand from Parangtritis Beach in Yogyakarta, Indonesia, was collected for this study. The chemicals used in the experiment include distilled water, hydrochloric acid (HCl 37% from Mallinckrodt), sodium hydroxide (NaOH from PA VWR Chemicals), silver nitrate (AgNO_3), pyridine (from Sigma Aldrich), dodecyl amine ($C_{12}H_{27}N$ from Fisher Scientific), and H_2 gas. Silica was synthesized from beach sand that contains SiO_2 [9].

2. General Procedure

a. Silica Extraction

Silica was synthesized from beach sand that contains SiO_2 [9]. The synthesis consists of washing the sand to remove excess Cl and impurities. The washed 10 g sands were then sieved with 100 mesh, refluxed with 6M HCl at 90 °C for four hours, filtered, and washed with distilled water until the pH was 7. The neutralized sand was then dried at 120 °C for two hours. Silica was extracted from the sand sample by refluxing each sample with 6M NaOH at a constant temperature of 80 °C for four hours, then filtered and washed. Concentrated HCl was then added dropwise into the filtrate until the pH reached 12 and the solution turned white. The solution was then stored for 24 hours until the gel was formed. Afterward, the gel separated and washed until the filtrate has no Cl. The synthesized silica was dried in an oven at 120 °C for four hours [5].

b. Mesoporous Silica Synthesis

Mesoporous silica was synthesized using n-dodecyl amine (DDA) surfactant as a template [12]. To obtain soluble sodium silicate, 2 g powdered SiO_2 was dissolved in a 45 mL NaOH solution 1.5 M and stirred at 40 °C for 30 minutes. The resulting mixture was adjusted to a pH of 5 by adding 6M H_2SO_4 until 8 was the solution pH.

In a separate step, a 0.25 M DDA solution was prepared by dissolving DDA in a 25 ml solvent mixture of distilled water and ethanol (1:1) at 40 °C for 30 minutes. The DDA solution was then subjected to dropwise addition of the sodium silicate solution under a rotation speed of 120 rpm at room temperature. The resulting solution was transferred into a hydrothermal reactor with an out diameter (OD)

of 10 cm, an inner diameter (ID) of 5 cm, and a 20 cm reactor height, and it was maintained at 100 °C for 12 hours.

After hydrothermal, the product was filtered, washed with distilled water until the filtrate reached a pH of 6, and dried at 50 °C for 4 hours. The dried product underwent calcination at 600 °C for 5 hours with a heating rate of 5 °C/min to remove the surfactant template. The experiment was repeated with varying time and DDA concentration as variables.

3. Characterization

Fourier-Transform Infrared Spectroscopy (FTIR) FTIR SHIMADZU Prestige 21 was utilized to analyze the silica samples, examining their functional groups and investigating the presence and elimination of the DDA template. To assess the acidity of sand, silica, and mesoporous silica, a gravimetric base adsorption method was employed, using pyridine as the base probe molecule. The acidity was determined through the following equation: the weight of adsorbed pyridine vapor (g), denoted as W C_5H_5N, divided by the weight of the mesoporous silica sample denoted as WY, and multiplied by the molecular weight of pyridine (79.01 g/mol) denoted as M C_5H_5N. The acidity was calculated with the following formula, where W C_5H_5N is the weight of adsorbed pyridine vapor (g), WY is the weight of mesopore silica, and Mr C_5H_5N is the molecular weight of pyridine (79.01 g/mol).

$$Acidity = \frac{WC_5H_5N}{W_Y M_{C_5H_5N}} \times 1000 \frac{mmol}{g} \text{ (1)}$$

The pore size and volume analysis was performed using N_2 gas sorption analysis, utilizing the Surface Area Analyzer Quantachrome NovaWin 1200e version 2.2. The adsorption and desorption isotherms were measured using the mul-

tipoint method. The total surface areas were calculated using the BET method, and the pore size distribution was determined using the BJH desorption model.

To evaluate the degree of crystallinity in the mesoporous silica, an X-ray diffraction (XRD) technique was employed. The Rigaku Miniflex 600 instrument was utilized for this analysis, utilizing a Cu Kα monochromatized radiation source with a wavelength of 1.54 Å. The XRD analysis was conducted under specific operating conditions, including 30 kV voltage and 10 mA current. The scan speed was set at 10°/min, and the scan range covered 2-80°

The morphology of the mesoporous silica was examined using both Scanning Electron Microscopy SEM-EDX JEOL JSM-6510, the analysis was carried out at the UGM Integrated Research and Testing Laboratory and Transmission Electron Microscopy Microscope JEOL-JEM-1400, the analysis was carried out at the Laboratory of Organic Chemistry, UGM Chemistry Department. These techniques allowed to characterize the pore structures within the mesoporous silica samples [9
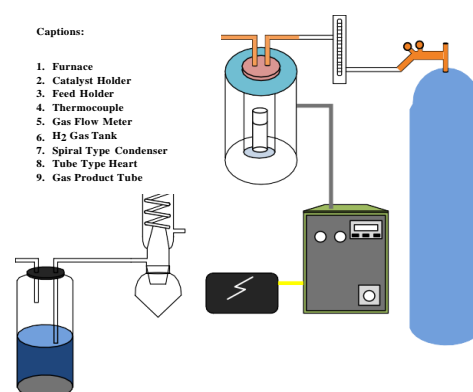
4. Hydrocracking Process

Figure 1. Hydrocracking reactor.

Hydrocracking of waste cooking oil was done by putting 0.1 g of MS and 10 g of waste cooking oil into the container. The waste cooking

oil sample and catalyst were put into a semi-fixed batch hydrocracking reactor. The reactor with OD 25 cm, ID = 5 cm, length = 40 cm, holder feed at 15 cm long, OD 5 cm. The oil sample and catalyst mixture were introduced into the hydrocracking reactor, as depicted in Figure 1. The reactor was then set to a temperature of 450 °C for 2 hours 1 atm, with a hydrogen gas flow rate of 20 ml/min.

The reactant conversion was determined gravimetrically by using calculation in the equation below [2]:

$$\text{Liquid fraction (LF) (wt.\%)} = \frac{\text{Wp}}{\text{WF}} \times 100\% \quad \textbf{(2)}$$

$$\text{Residue (wt.\%)} = \frac{\text{WR}}{\text{WF}} \times 100\% \quad \textbf{(3)}$$

$$\text{Coke (wt.\%)} = \frac{\text{WC2} - \text{WC1}}{\text{WF}} \times 100\% \quad \textbf{(4)}$$

$$\text{Gas} = 100 - (\text{LF} + \text{coke} + \text{residue}) \quad \textbf{(5)}$$

$$\text{Total result (\%)} = (100 - \text{residue}) \quad \textbf{(6)}$$

Where Wp is the weight of the product, WF is the weight feed, WR is the unconverted weight product (g), WC1 is the weight of the catalyst before hydrotreatment (g), and WC2 is the weight of the catalyst after hydrocracking (g).

RESULTS AND DISCUSSION

1. Synthesis of mesoporous silica

To extract silica from beach sand, 2 grams of powdered SiO_2 were dissolved in 45 mL of 1.5 M NaOH solution and stirred at 40 °C for 30 minutes. The resulting mixture had its pH adjusted to 5 by adding 6 M H_2SO_4 until the solution's pH reached 8. The precipitated H_2SiO_3 was then separated through filtration. Subsequently, the precipitated silica was dried at 50°C for 4 hours to remove water molecules, resulting in a brittle white powder of silica oxide (SiO_2). This SiO_2 was easily crushed and further used in synthesizing mesoporous silica (MS) with Dodecylamine (DDA) templates using the hydrothermal method.

Dodecylamine (DDA), as a template in synthesizing mesoporous silica, plays a vital role in forming the desired pore structure. DDA allows for control over the pore size of the resultant mesoporous silica. This pore size can be fine-tuned by varying the DDA concentration. The template also aids in preventing the collapse of the mesoporous structure during synthesis, resulting in a higher surface area.
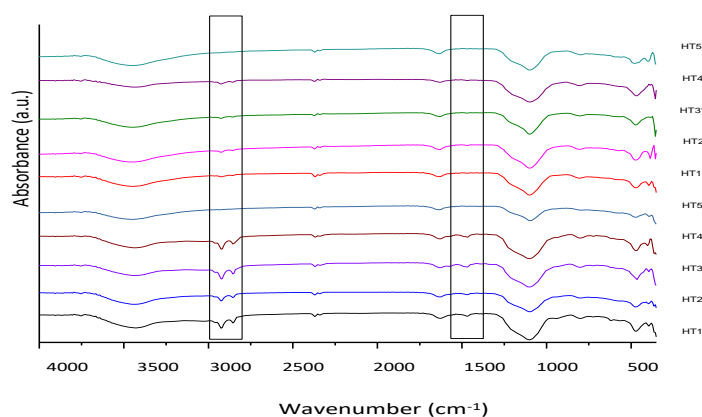

Figure 2. Hydrothermal FTIR spectra before calcination (HT) and after calcination (HT*).

The hydrothermal process involved variations in the duration of hydrothermal treatment and the DDA concentration. The synthesized silica was divided into five samples for studying hydrothermal time: MSHT1 (hydrothermalized for 12 hours), MSHT2 (15

hours), MSHT3 (18 hours), MSHT4 (21 hours), and MSHT5 (24 hours). Subsequently, the mesoporous silica samples were calcined and denoted as MSHT*. Additionally, mesoporous silica synthesis was conducted with varying DDA concentrations, yielding three samples: MSA, MSB, and MSC. The synthesized mesoporous silica was subjected to FTIR analysis for characterization, with the results presented in Figure 2.

The absorption spectra depicted in Figure 2 reveal various functional groups in the mesoporous silica (MS). Within the wavenumber range of 500 cm^{-1} to 4000 cm^{-1}, broad bands can be observed, indicating the presence of Si, O, and H functional groups. The spectra at wavenumbers 799.67 cm^{-1} and 941 cm^{-1} suggest Si-O-Si stretching, indicating the formation of silicon-oxygen-silicon bonds. Additionally, the presence of a Si-O-Si group is indicated by the peak observed at wavenumber 1103 cm^{-1} [13,19].

The spectra exhibit a peak at wavenumber 1465 cm^{-1}, indicating the presence of a primary amine group and corresponding to N-H stretching vibrations. Similarly, the peak observed at wavenumber 3425 cm^{-1} represents the vibration of N-H stretching for the primary amine group. These observations suggest that the dodecyl amine template is coated with silica, as demonstrated by the interaction between the amine group and the silica framework. The observations made in this study provide evidence that the dodecyl amine template is indeed coated with silica. This is indicated by the interaction observed between the amine group of the template and the silica framework. The presence of the amine group in the dodecyl amine template allows for its interaction with the surface of the silica material. Silica, composed of silanol groups (Si-OH) on its surface, can form hydrogen bonds with the amine group (-NH$_2$) of the dodecyl amine template. This interaction leads to the coating of the amine template with silica, as confirmed by the absorption spectra.

Figure 2 reveals notable observations regarding peak losses in the HT* sample at wavenumbers 1465 cm^{-1} and 3425 cm^{-1}. These peak losses indicate the dissociation of N-H bonds from the mesoporous silica framework, aligning with the findings reported in [20], which also observed the detachment of N-H groups from similar mesoporous silica materials.

The dissociation of N-H bonds from the mesoporous silica framework can be attributed to several factors. A primary consideration is the desorption or removal of amine groups during calcination, where the samples are exposed to high temperatures. This heating might result in the decomposition or volatilization of the amine groups, leading to the detachment of N-H bonds from the silica structure. Additionally, the structural changes in the mesoporous silica during hydrothermal and calcination processes might also contribute to this detachment. These processes could cause rearrangement or reorganization within the silica framework, disrupting certain chemical bonds, including N-H bonds.

The findings related to the coating of the dodecylamine template with silica and the separation of N-H bonds from the mesoporous silica framework provide critical insights into the interactions and transformations within the synthesized materials. Further investigation is necessary to fully understand the mechanisms and implications of these observations. The absorption peak at wavenumber 3448.7 cm^{-1} suggests the presence of -OH stretching vibrations, which are associated with silanol groups on the mesoporous silica surface [19].

Other research in the field of mesoporous silica synthesis supports our methodology. For example, a study utilized the sol-gel method to synthesize mesoporous silica nanoparticles, demonstrating the preparation of silica particles through controlled hydrolysis of TEOS as a silica precursor [21]. These studies validate our approach and provide a more comprehensive understanding of the synthesis methods and materials used in mesoporous silica research.

2. Acidity Test

The role of acidity in mesoporous materials is paramount, especially in the realm of catalytic applications. Mesoporous materials that feature both Lewis acid sites (LAS) and Brønsted acid sites (BAS) are increasingly utilized in various acid-catalyzed reactions. Their applicability stems from attributes such as high thermal stability, consistent pore sizes, and expansive pore volumes [21]. Assessing the acidity of mesoporous silica is particularly critical in determining the catalyst's efficiency in hydrocracking processes, where the acidity directly influences the catalyst's activity and selectivity.

Acidity testing is instrumental in understanding the surface interactions within mesoporous materials. These acidic sites are active participants in a plethora of chemical reactions and adsorption processes. By comparing the acidity levels of various materials, researchers can make more informed selections, choosing materials best suited for specific applications based on their acidity characteristics. Such tests are pivotal for enhancing catalytic processes, understanding surface interactions, and aiding in the selection of materials.

In this study, the acid sites on the surface of mesoporous silica (MS) were identified using a gravimetric approach in the acidity test. This method involves measuring the weight change of a catalyst sample before and after exposure to an adsorbate, in this case, pyridine vapor. The test was conducted under vacuum conditions, and the results, encompassing acidity measurements for silica and mesoporous silica, are displayed in Table 1.

Table 1. The acidity of silica and mesoporous silica during hydrothermal variation

Sample	Acidity (mmol/gr)
Silica	1.13
MSHT1	1.38
MSHT2	1.67
MSHT3	1.74
MSHT4	1.61
MSHT5	1.48

The data from Table 1 reveals that the hydrothermal duration significantly impacts the acidity of mesoporous silica (MS). An increase in hydrothermal time generally leads to an increase in acidity, with the peak at 18 hours (MSHT3) showing an acidity value of 1.74 mmol/g. However, beyond this optimum duration, a decline in acidity is observed. This trend could be attributed to a decrease in accessible acidity sites, possibly due to reduced pore accessibility or pore shrinkage, as hypothesized in previous studies [9]. These findings underscore that MS exhibits greater overall acidity than conventional silica, rendering it a promising candidate for catalytic applications, especially in metal-bearing catalysts.

3. Characterization of Mesoporous Silica with a Gas Sorption Analyzer (GSA)

The Gas Sorption Analyzer (GSA) technique is critical for determining materials' specific surface area, pore volume, and pore size distribution. This method involves the adsorption of gases, such as nitrogen or carbon dioxide, onto

the surface of the analyzed material. In the context of mesoporous materials, the specific surface area and pore volume are essential characteristics, especially for catalytic applications. A higher specific surface area indicates increased active sites for reactant

interaction with the catalyst. Similarly, the pore volume of mesoporous materials is crucial, as it influences the material's adsorption capacity and its ability to host reactants or molecules of interest.

Table 2. Characteristics of mesoporous silica synthesized using hydrothermal method

Material	Surface area (m²/g)	Total pore volume (cc/g)	Pore diameter (nm)
Sand	1.08	0.003	2.43
Silica	17.8	0.06	2.43
MSHT1	127	0.33	2.54
MSHT2	172.5	0.48	6.62
MSHT3	158.1	0.34	5.19
MSHT4	157.1	0.56	8.75
MSHT5	136.9	0.40	2.20
MSA	233.4	0.47	2.10
MSB	151.6	0.59	10.43
MSC	142.97	0.24	2.10

Table 2 presents the findings from an analysis of the specific surface area and pore volume of synthesized mesoporous silica (MS). The surface area of MS was ascertained using N_2 gas adsorption-desorption isotherm data, applying the Brunauer-Emmett-Teller (BET) method. Additionally, the analysis of pore volume and pore size distribution was conducted using N_2 gas desorption data from the MS surface, employing the Barrett-Joyner-Halenda (BJH) method.

These characterization techniques confirm the mesoporous properties of the synthesized MS, providing valuable insights into its pore formation and size distribution, with a particular focus on pore diameter. According to the material categorization criteria outlined in [13], the results of this analysis facilitate the classification of the mesoporous material based on its pore size. Such classification is essential in assessing the suitability of the material for various applications, especially in catalysis, where the pore structure significantly influences performance efficiency.

Mesoporous silica samples A, B, and C, corresponding to DDA concentrations of 0.25 M, 0.5 M, and 0.1 M respectively, were analyzed. Table 2 reveals increased surface area for sand, silica, and mesoporous silica. The sand sample exhibits a surface area of 1.08 m^2/g and contains various metals and impurities. The diameter measurements indicate that the sand possesses mesoporous characteristics [5]. Among the mesoporous silica samples, MSHT2, synthesized with a hydrothermal time of 15 hours, exhibits the largest specific surface area. As the hydrothermal time increases, the surface area and diameter tend to decrease, except in MSHT4, where the diameter increases. It could be attributed to structural changes that occur during the longer synthesis time, affecting the distribution of pores. The decreasing trend in acidity test results supports this observation. The hydrothermal time represents the preparation process for micelle formation, and after the optimal formation process, further increases in hydrothermal time have limited effects [10].
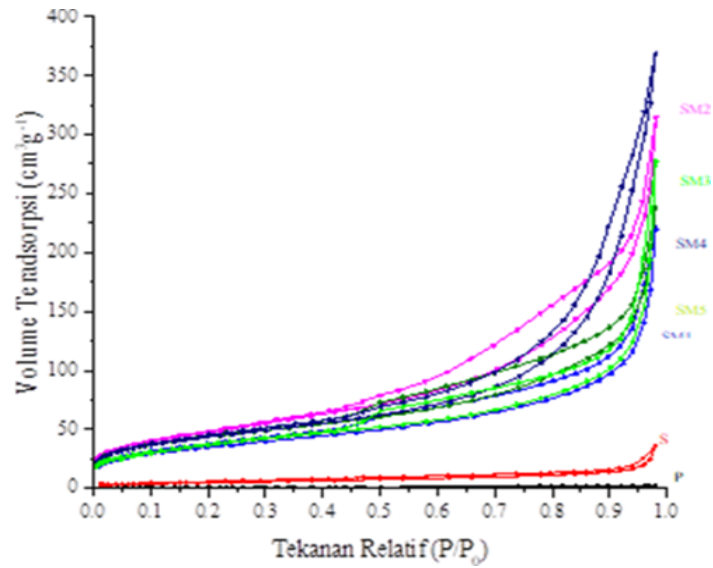
Figure 3. Adsorption and desorption of sand (P), silica (S), and mesoporous silica from hydrothermal process (MS).
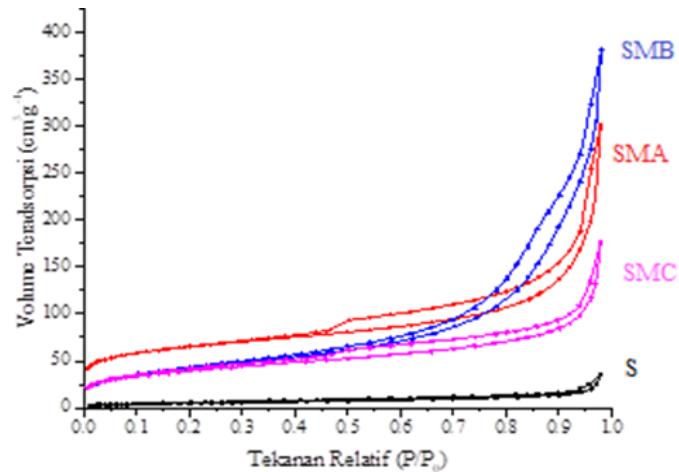

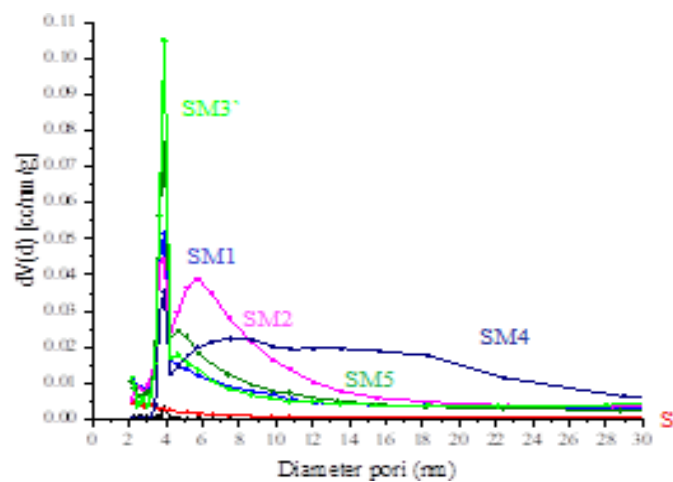**Figure 4.** Adsorption and desorption of silica and mesoporous silica with DDA concentration as a variable.

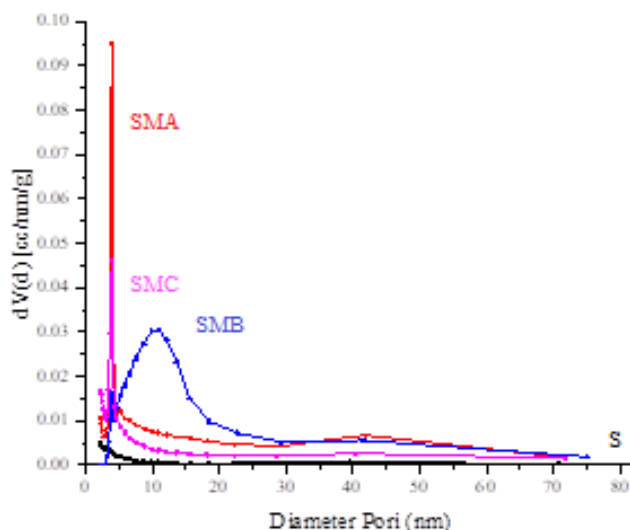**Figure 5.** Distribution of pore mesoporous silica with hydrothermal time as a variable.

Figure 6. The pore distribution of mesoporous silica with DDA concentration as a variable.

The analysis of mesoporous silica with varying DDA concentrations reveals that higher template concentrations lead to lower surface areas. The ideal critical micelle concentration (CMC) causes this effect at a DDA concentration of 0.05. The CMC conditions significantly determine the state and structure of the pores formed [5]. Table 2 displays the results of pore size analysis for the synthesized mesoporous silica, indicating a range of 2-50 nm, which confirms the desired mesoporous properties of the material. The adsorption-desorption graphs are depicted in Figures 3 and 4.

The N_2 gas adsorption-desorption isotherm graph for mesoporous silica displays a hysteresis loop with slightly different pressures for each material, aligning with the IUPAC type IV isotherm pattern [5,22]. All five materials demonstrate mesoporous characteristics, characterized by a hysteresis loop where the desorption and adsorption curves converge at relatively low P/P_0 ratios, indicating an uneven distribution of pore sizes. Figure 3 shows the impact of DDA concentration on the adsorption and desorption graphs for MS B, which also exhibits a

hysteresis loop following the IUPAC type IV isotherm pattern, suggesting a more uniform pore distribution. For MSC, the surface area is reported as 142.97 m^2/g, with a pore diameter of only 2.1 nm.

The pore size distribution of mesoporous silica is illustrated in Figures 4 and 5, with pore sizes ranging from 2 to 30 nm, consistent with the standard mesoporous material pore size range of 2–50 nm [23]. The mesoporous properties of the synthesized mesoporous silica (MS) are thus confirmed by the observed pore size distribution.

Figure 4 reveals that MSHT1 has a pore distribution primarily in the 2-4 nm range, distinguishing it from MSHT2, which displays a larger surface area and a more uniform distribution of pores. In terms of varying DDA concentrations, the black color in the graph represents the silica distribution. MSA shows a surface area of 233.4 m^2/g and a considerable number of pores, as indicated by a d/v pore volume close to 0.1. As the DDA concentration increases, there is a more pronounced accumulation of pores, leading to a decrease in surface area [15].

4.   The Crystallinity of Mesoporous Silica

Amorphous structures in mesoporous materials are crucial in various applications, particularly in catalysis. The high surface area and suitable pore size of these materials make them ideal for catalytic applications, adsorption, and separation processes [24]. The crystallinity of mesoporous silica (MS) is determined through X-ray diffraction (XRD) analysis, which provides essential insights into its structure. As indicated in Figure 7, the XRD results reveal that the synthesized MS possesses an amorphous structure. This observation aligns with findings from previous studies, which have also reported the amorphous nature of mesoporous silica [13,16,25]. The amorphous configuration of mesoporous silica indicates a lack of long-range order in its structure, consisting of randomly arranged particles.

The amorphous nature of mesoporous silica (MS) is crucial for its potential applications across various fields. Amorphous materials are characterized by a high degree of structural disorder, which imparts unique properties such as a large surface area, enhanced catalytic activity, and superior adsorption capabilities. The lack of a well-defined crystal structure in amorphous materials allows for more accessible active sites, thereby facilitating efficient adsorption and reaction processes.
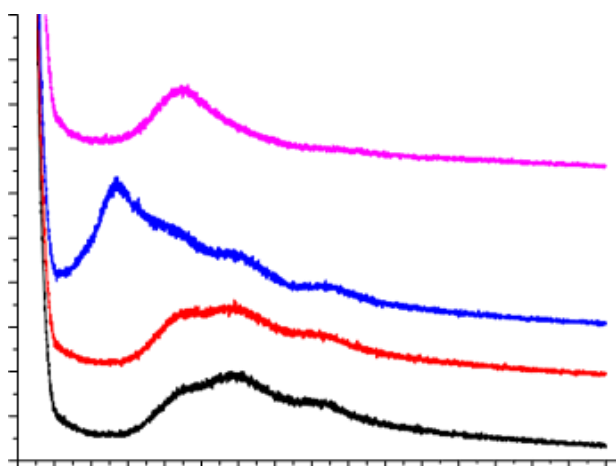

Figure 7. XRD Diffractogram of MSHT.

The impact of hydrothermal time on the amorphous character of MS is evident in the X-ray diffraction (XRD) data. The data indicate that the intensity of the amorphous phase increases with prolonged hydrothermal treatment, as observed in samples MSHT3 and MSHT4. This observation aligns with existing research, suggesting that extended hydrothermal treatment enhances the amorphous nature of the mesoporous structure [10].

The amorphous state of MS, particularly in the form of a Hexa-mesoporous structure, holds great promise for applications in various fields. The absence of well-defined crystal planes allows for greater flexibility in tailoring the material's pore size, surface area, and functionalization to suit specific needs. The amorphous nature also facilitates the incorporation of various guest species or functional groups within the mesoporous framework, enabling the design of advanced materials for diverse applications such as drug delivery, gas adsorption, and catalysis.

In summary, the XRD analysis confirms that the synthesized mesoporous silica (MS) exhibits an amorphous structure consistent with previous studies. The amorphous nature of MS offers unique advantages, including high surface area, improved catalytic activity, and versatile functionalization possibilities. The influence of hydrothermal time on the amorphous character further emphasizes the potential for tailoring the properties of MS for specific applications. Further research can explore the relationship between the amorphous structure, pore characteristics, and the performance of MS in various applications.

## 5. Characterization of mesoporous silica by SEM and TEM

Scanning Electron Microscopy (SEM) analysis plays a pivotal role in assessing the surface morphology of synthesized mesoporous silica (MS). The micrograph in Figure 8 shows small grains that constitute a mesoporous structure, suggestive of narrow pores arranged uniformly. This structural observation is consistent with similar findings from previous studies on MSHT [10]. Additional insights into the pore surface morphology are provided in Figure 9.
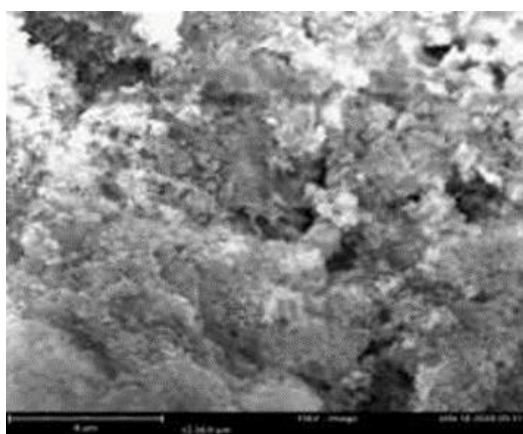
(a)
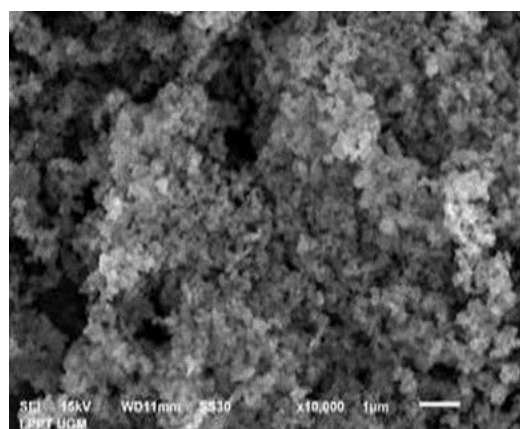
(b)
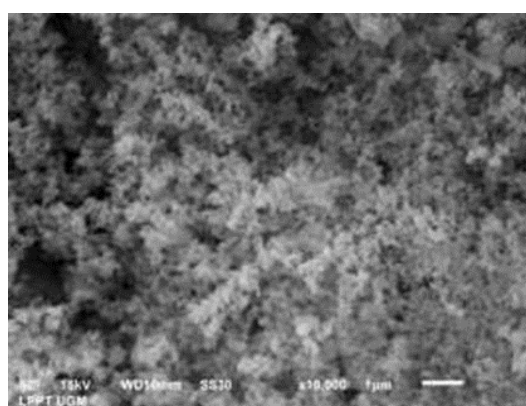
(c)

Figure 8. SEM images of (a) silica, (b) MSHT3, and (c) MSB.

A Transmission Electron Microscopy (TEM) image is essential to corroborate the pore structure observed in SEM. Figure 9 presents a TEM image of MSHT3, revealing

visible pore gaps that resemble wormholes. Using Dodecylamine (DDA) as a non-ionic template contributes to an irregular pore structure in MS [12]. In MSHT3, pore-blocking leads to a reduced pore surface area, as evidenced by the Gas Sorption Analyzer (GSA) analysis results in Table 2. A similar trend is observed with increased DDA concentration in MSB and MSC, resulting in a less regular pore structure and pore-blocking. This trend is evident from the observed decrease in acidity, surface area, pore distribution, and diameter changes. Among these materials, MSB exhibits the highest pore diameter compared to MSA and MSC, aligning with findings from previous studies [5,16].

These morphological and structural analyses provide valuable insights into the characteristics of the synthesized mesoporous silica. The SEM images confirm the presence of small-grained mesoporous structures with uniform pores, while the TEM images validate the presence of wormhole-like pores. The irregular pore structure observed in MS, influenced by the DDA concentration, indicates the complexity of pore formation and the occurrence of pore-blocking phenomena. These findings shed light on the interplay between synthesis conditions, pore morphology, and surface properties of mesoporous silica, offering opportunities for tailoring their characteristics for specific applications. Further investigations can explore the relationship between pore structure, pore size distribution, and the performance of mesoporous silica in various applications.
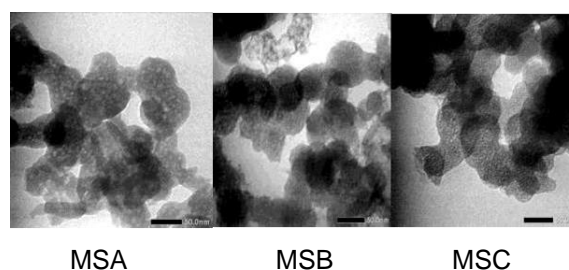

MSHT3

MSA   MSB   MSC
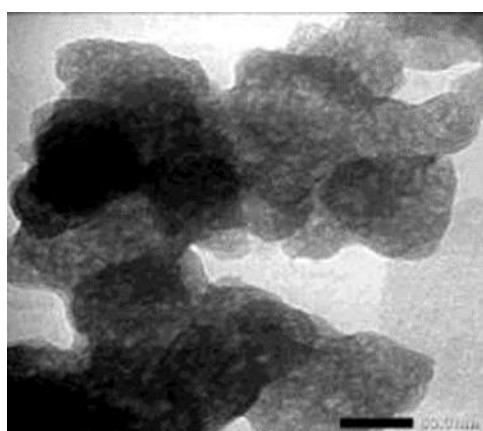
Figure 9. TEM images of mesoporous silica synthesized by hydrothermal.

To validate the presence of pore gaps in the synthesized mesoporous silica (MS) as indicated by the Grain Size Analysis (GSA) results, a Transmission Electron Microscopy (TEM) image is essential. Figure 9, showing the MSHT3 sample, reveals distinct pore structures that resemble wormholes. Using Dodecylamine (DDA) as a non-ionic template has led to an irregular pore structure in MS, resulting in wormhole-like pore configurations [12]. For the MSHT3 sample, pore-blocking is observed, leading to a decrease in pore surface area, as detailed in the GSA analysis results presented in Table 2. A similar pattern is noted with increasing DDA concentration in SMB and MSC, characterized by a less regular pore

structure and pore-blocking. This is evident from the decreased acidity and surface area and the pore distribution image and pore diameter. Among these materials, MSB exhibits the largest pore diameter compared to MSA and MSC, which is consistent with previous research findings [5,15].

6. Catalyst Activity

The synthesized mesoporous silica catalyst has been applied in the cracking process of used cooking oil, aiming to convert fatty acids into hydrocarbons. This application is significant as it offers enhanced stability and calorific value, making the oil suitable for transportation [16]. The hydrocracking process of used cooking oil involves the conversion of the oil into liquid, gas, and coke fractions, as presented in Table 3.

During thermal cracking, the production of the liquid fraction is relatively limited, while a substantial amount of residue is generated. However, when using the hydrocracked sand catalyst with a smaller surface area, the resulting residue reaches 56.74%. On the other hand, MSHT1, which possesses a larger surface area compared to the different time variables, demonstrates superior cracking performance. The catalyst's characteristics align with these findings.

Table 3. The product distribution of used cooking oil hydrocracked with a catalyst

| Parameters | Catalyst | | | | | | | | |
| | Product Distribution | | | | | | | | |
	Thermal	Sand	HT1	HT2	HT3	HT4	MSA	MSB	MSC
Liquid Fraction (%w)	41.3	19.41	70.23	62.19	41.94	49.34	71.59	64.7	71.3
Gas Fraction (%w)	25.86	22.97	26.69	36.6	38.76	42	26	33.05	10
Coke (%w)	0.55	0.88	0.1	0.24	0.21	0.02	0.6	0.1	0.1
The residue (%w)	32	56.74	29	0.95	19	8.3	1.7	1.5	18

Regarding catalysts with varying DDA concentrations, it is observed that higher DDA concentrations lead to less supportive catalyst characteristics, resulting in less efficient cracking. However, mesoporous silica synthesized through an optimal hydrothermal process involving appropriate hydrothermal time and DDA concentration exhibit superior performance. As the relatively low gas fraction generated indicates, it can efficiently produce a significant liquid fraction while minimizing excessive cracking. This behavior can be attributed to the excellent pore structure of the catalyst. Mesopores on the catalyst's surface allow for efficient feed penetration, enabling rapid product release. In contrast, during thermal cracking, the production of the liquid fraction is relatively limited, while the residue fraction is more substantial.

The application of mesoporous silica catalysts in the cracking process of used cooking oil holds promise for the production of valuable hydrocarbon fractions with improved stability and calorific value. The superior performance of mesoporous silica catalysts, especially those synthesized through an optimized hydrothermal process, showcases the importance of pore structure and surface characteristics in achieving desired cracking outcomes. Further investigations can explore

the optimization of process parameters, catalyst design, and feedstock properties to enhance the efficiency and selectivity of the cracking process, contributing to the development of sustainable and efficient energy conversion technologies.

Due to its elevated porosity, Mesoporous silica exhibits a heightened propensity for coke accumulation compared to conventional silica. This material also demonstrates significantly higher acidity, as determined through pyridine gas adsorption, surpassing silica and sand. The alkane/alkene ratio in mesoporous silica is notably lower than that in silica, which can be attributed to the deeper location of acid sites within the mesoporous structure. This characteristic facilitates swift ingress and egress of feed and product molecules, minimizing the likelihood of feed molecules encountering an active site within the catalyst before exiting.

The mesoporous structure is crucial in selecting desired fuel fractions despite appearing less favorable for cracking reactions in used cooking oil. The hydrodeoxygenation mechanism in mesoporous silica efficiently removes oxygen from fatty acids, such as C18 and C16, found in used cooking oil while preserving carbon content. This process results in the retention of longer-chain hydrocarbons with higher molecular weights [15]. These properties indicate that the synthesized mesoporous silica possesses strong desorption capabilities, promoting the efficient release of products from the catalyst and supporting the formation of diesel or premium oil fractions.

Consequently, the catalyst facilitates rapid movement of feed and product molecules, reducing the chance of interaction with active sites. Future investigations could optimize catalyst design and operational conditions to enhance fuel fraction yield and overall cracking efficiency, contributing significantly to sustainable energy conversion processes.

CONCLUSION

The hydrothermal method has been effectively utilized to synthesize mesoporous silica from beach sand, achieving notable characteristics. This synthesized mesoporous silica exhibits an acidity of 0.88 mmol/g and optimizes at a hydrothermal duration of 15 hours. Key properties include a surface area of 172.5 m²/g, pore volume of 0.42 cc/g, and pore diameter of 6.62 nm. When varying dodecyl amine (DDA) concentration shows enhanced characteristics with a surface area of 233 m²/g, pore volume of 0.47 cc/g, and an average pore diameter of 2.10 nm. These properties make the mesoporous silica an effective catalyst for hydrocracking used cooking oil, yielding high liquid fractions of 70.23% and 71.59%. This underlines its potential as a catalyst in converting used cooking oil into valuable hydrocarbons, contributing to sustainable and eco-friendly fuel production methods. Further research could optimize hydrocracking parameters to improve the yield and quality of the liquid fraction, enhancing mesoporous silica's application in renewable energy production.

ACKNOWLEDGMENT

REFERENCES

[1] P. Yotsomnuk and W. Skolpap, "Effect of process parameters on yield of biofuel production from waste virgin coconut oil," *Eng. J.*, vol. 22, no. 6, pp. 21–35, 2018, doi: 10.4186/ej.2018.22.6.21.

[2] S. Salamah, W. Trisunaryanti, I. Kartini, and S. Purwono, "Synthesis of Mesoporous Silica from Beach Sand by Sol-Gel Method as a Ni Supported Catalyst for Hydrocracking of Waste Cooking Oil," *Indones. J. Chem.*, vol. 22, no. 3, pp. 726–741, 2022, doi: 10.22146/ijc.70415.

[3] L. Badriyah and I. I. Falah, "Gasoline Production from Coconut Oil Using The Ni-MCM-41 and Co/Ni-MCM-41 Catalyst," *JKPK (Jurnal Kim. Dan Pendidik. Kim.*, vol. 2, no. 1, p. 22, 2017, doi: 10.20961/jkpk.v2i1.8516.

[4] D. G. Ramadhani, A. W. Sarjono, H. Setyoko, N. F. Fatimah, and N. D. Nurhayati, "Synthesis of Natural Ni/Zeolite Activated by Acid as Catalyst for Synthesis Biodiesel from Ketapang Seeds Oil," *JKPK (Jurnal Kim. Dan Pendidik. Kim.*, vol. 2, no. 1, p. 72, 2017, doi: 10.20961/jkpk.v2i1.8530.

[5] A. S. Golezani, A. S. Fateh, and H. A. Mehrabi, "Synthesis and characterization of silica mesoporous material produced by hydrothermal continues pH adjusting path way," *Prog. Nat. Sci. Mater. Int.*, vol. 26, no. 4, pp. 411–414, 2016, doi: 10.1016/j.pnsc.2016.07.003.

[6] M. Ulfa, W. Trisunaryanti, I. I. Falah, and I. Kartini, "Influence of Time and Concentration on Textural Properties of Mesoporous Carbons of Gelatin Prepared By Hard-Templating Process," *JKPK (Jurnal Kim. dan Pendidik. Kim.*, vol. 1, no. 1, p. 1, 2020, doi: 10.20961/jkpk.v1i1.10126.

[7] K. Wijaya, A. Nadia, A. Dinana, A. F. Pratiwi, A. D. Tikoalu, and A. C. Wibowo, "Catalytic hydrocracking of fresh and waste frying oil over ni-and mo-based catalysts supported on sulfated silica for biogasoline production," *Catalysts*, vol. 11, no. 10, 2021, doi: 10.3390/catal11101150.

[8] S. Salamah, W. Trisunaryanti, I. Kartini, and S. Purwono, "Synthesis and characterization of mesoporous silica from beach sands as silica source," *IOP Conf. Ser. Mater. Sci. Eng.*, vol. 1053, no. 1, p. 012027, 2021, doi:10.1088/1757-899x/1053/1/012027.

[9] H. Y. Lin and Y. W. Chen, "Preparation of spherical hexagonal mesoporous silica," *J. Porous Mater.*, vol. 12, no. 2, pp. 95–105, 2005, doi: 10.1007/s10934-005-6766-y.

[10] R. Thahir, A. W. Wahab, N. La Nafie, and I. Raya, "Synthesis of high surface area mesoporous silica SBA-15 by adjusting hydrothermal treatment time and the amount of polyvinyl alcohol," *Open Chem.*, vol. 17, no. 1, pp. 963–971, 2019, doi: 10.1515/chem-2019-0106.

[11] R. Filipović, Z. Obrenović, I. Stijepović, L. M. Nikolić, V. V. Srdić, "Synthesis of mesoporous silica particles with controlled pore structure," *Ceramics International*, vol. 35, no. 8, pp. 3347–3353, 2009, doi: 10.1016/j.ceramint.2009.05.040.

[12] S. Lin *et al.*, "Direct synthesis without addition of acid of Al-SBA-15 with controllable porosity and high hydrothermal stability," *Microporous Mesoporous Mater.*, vol. 142, no. 2–3, pp. 526–534, 2011, doi: 10.1016/j.micromeso.2010.12.043.

[13] F. Kooli, Y. Liu, K. Hbaieb, and R. Al-Faze, "Characterization and catalytic properties of porous clay heterostructures from zirconium intercalated clay and its pillared derivatives," *Microporous Mesoporous Mater.*, vol. 226, pp. 482–492, 2016, doi: 10.1016/j.micromeso.2016.02.025.

[14] S. Salamah, A. Aktawan, and I. Mufandi, "The Characterization of Synthetic Zeolite for Hydrocracking of Waste Cooking Oil into Fuel," *Reaktor*, vol. 20, no. 2, pp. 89–95, 2020, doi: 10.14710/reaktor.20.2.89-95.

[15] W. Trisunaryanti, S. Larasati, T. Triyono, N. R. Santoso, and C. Paramesti, "Selective production of green hydrocarbons from the

hydrotreatment of waste coconut oil over Ni- And NiMo-supported on amine-functionalized mesoporous silica," *Bull. Chem. React. Eng. Catal.*, vol. 15, no. 2, pp. 415–431, 2020, doi: 10.9767/bcrec.15.2.7136.415-431.

[16] Hartati *et al.*, "Highly selective hierarchical ZSM-5 from kaolin for catalytic cracking of Calophyllum inophyllum oil to biofuel," *J. Energy Inst.*, vol. 93, no. 6, pp. 2238–2246, 2020, doi: 10.1016/j.joei.2020.06.006.

[17] G. D. Alisha, W. Trisunaryanti, and A. Syoufian, "Mesoporous Silica from Parangtritis Beach Sand Templated by CTAB as a Support of Mo Metal as a Catalyst for Hydrocracking of Waste Palm Cooking Oil into Biofuel," *Waste and Biomass Valorization*, vol. 13, no. 2, pp. 1311–1321, 2022, doi: 10.1007/s12649-021-01559-y.

[18] A. Yıldız, J. L. Goldfarb, and S. Ceylan, "Sustainable hydrocarbon fuels via 'one-pot' catalytic deoxygenation of waste cooking oil using inexpensive, unsupported metal oxide catalysts," *Fuel*, vol. 263, no. December 2019, p. 116750, 2020, doi: 10.1016/j.fuel.2019.116750.

[19] A. Aneu, K. Wijaya, and A. Syoufian, "Silica-Based Solid Acid Catalyst with Different Concentration of H_2SO_4 and Calcination Temperature: Preparation and Characterization," *Silicon*, vol. 13, no. 7, pp. 2265–2270, 2021, doi: 10.1007/s12633-020-00741-6.

[20] J. Q. Dalagan and E. P. Enriquez, "One-step synthesis of mesoporous silica-graphene composites by simultaneous hydrothermal coupling and reduction of graphene oxide," *Bull. Mater. Sci.*, vol. 37, no. 3, pp. 589–595, 2014, doi: 10.1007/s12034-014-0661-6.

[21] H. Xu *et al.*, "Correlation between Acidity and Catalytic Performance of Mesoporous Zirconium Oxophosphate in Phenylglyoxal Conversion," *ACS Sustain. Chem. Eng.*, vol. 7, no. 9, pp. 8931–8942, 2019, doi: 10.1021/acssuschemeng.9b00989.

[22] F. Sotomayor, A. P. Quantatec, F. J. Sotomayor, K. A. Cychosz, and M. Thommes, "Characterization of Micro/Mesoporous Materials by Physisorption: Concepts and Case Studies," *Acc. Mater. Surf. Res*, vol. 3, no. 2, pp. 34–50, 2018.

[23] S. Nuntang, S. Yousatit, T. Yokoi, and C. Ngamcharussrivichai, "Tunable mesoporosity and hydrophobicity of natural rubber/hexagonal mesoporous silica nanocomposites," *Microporous Mesoporous Mater.*, vol. 275, pp. 235–243, 2019, doi: 10.1016/j.micromeso.2018.09.004.

[24] Z. A. Alothman, "A review: Fundamental aspects of silicate mesoporous materials," *Materials (Basel).*, vol. 5, no. 12, pp. 2874–2902, 2012, doi: 10.3390/ma5122874.

[25] L. Cheng, J. Cai, and Y. Ke, "Synthesis of Large-Pore Silica Microspheres Using Dodecylamine as a Catalyst, Template and Porogen Agent," *J. Inorg. Organomet. Polym. Mater.*, vol. 29, no. 4, pp. 1417–1421, 2019, doi: 10.1007/s10904-019-01086-3.